RESEARCH ONLINE

University of Wollongong
Research Online

Faculty of Science - Papers (Archive)

Faculty of Science, Medicine and Health

2011

Gellan gum doped polypyrrole neural prosthetic electrode coatings

Thomas M. Higgins

Simon E. Moulton
University of Wollongong, smoulton@uow.edu.au

Kerry J. Gilmore
University of Wollongong, kerryg@uow.edu.au

Gordon G. Wallace
University of Wollongong, gwallace@uow.edu.au

Marc in het Panhuis
University of Wollongong, panhuis@uow.edu.au

Publication Details

Higgins, T. M., Moulton, S. E., Gilmore, K. J., Wallace, G. G. & in het Panhuis, M. (2011). Gellan gum doped polypyrrole neural prosthetic electrode coatings. Soft Matter, 7 (10), 4690-4695.

Research Online is the open access institutional repository for the University of Wollongong. For further information contact the UOW Library: research-pubs@uow.edu.au

RESEARCH ONLINE

Gellan gum doped polypyrrole neural prosthetic electrode coatings

Abstract

Surface modification of neural prosthetic electrodes with polymeric materials, in particular, conducting polymers and hydrogels, has the potential to circumvent many problems associated with currently used electrode platforms. These problems include the disparity in mechanical properties between implanted electrodes and host neural tissue and the lack of biofunctionality at the electrode surface, both of which dissuade favourable reception of the implanted device. We have developed conducting polymer electrode coatings doped with the polysaccharide gellan gum, as a platform for improved functionality of neural prosthetic electrodes. Our electrode coatings, prepared by galvanostatic electropolymerisation, significantly reduced the impedance magnitude at frequencies relevant to neural cells, relative to uncoated gold Mylar electrodes (24 3 U at 1 kHz). Cyclic voltammetry was used to explore the electrochemical stability of the coatings, which lose only 23 2% charge carrying capacity when subjected to 400 redox cycles. The coatings show no change in impedance magnitude at 1 kHz when subject to 32 h of clinically relevant charge balanced current stimulation.

Keywords

gellan, coatings, electrode, prosthetic, neural, polypyrrole, doped, gum

Disciplines

Life Sciences | Physical Sciences and Mathematics | Social and Behavioral Sciences

Publication Details

Higgins, T. M., Moulton, S. E., Gilmore, K. J., Wallace, G. G. & in het Panhuis, M. (2011). Gellan gum doped polypyrrole neural prosthetic electrode coatings. Soft Matter, 7 (10), 4690-4695.

This journal article is available at Research Online: http://ro.uow.edu.au/scipapers/1015

Soft Matter

Dynamic Article Links

Cite this: *Soft Matter*, 2011, **7**, 4690

www.rsc.org/softmatter

PAPER

Gellan gum doped polypyrrole neural prosthetic electrode coatings

Thomas M. Higgins,[ab] Simon E. Moulton,[a] Kerry J. Gilmore,[a] Gordon G. Wallace*[a] and Marc in het Panhuis*[ab]

Received 15th January 2011, Accepted 4th March 2011
DOI: 10.1039/c1sm05063j

Surface modification of neural prosthetic electrodes with polymeric materials, in particular, conducting polymers and hydrogels, has the potential to circumvent many problems associated with currently used electrode platforms. These problems include the disparity in mechanical properties between implanted electrodes and host neural tissue and the lack of biofunctionality at the electrode surface, both of which dissuade favourable reception of the implanted device. We have developed conducting polymer electrode coatings doped with the polysaccharide gellan gum, as a platform for improved functionality of neural prosthetic electrodes. Our electrode coatings, prepared by galvanostatic electropolymerisation, significantly reduced the impedance magnitude at frequencies relevant to neural cells, relative to uncoated gold Mylar electrodes (24 ± 3 Ω at 1 kHz). Cyclic voltammetry was used to explore the electrochemical stability of the coatings, which lose only 23 ± 2% charge carrying capacity when subjected to 400 redox cycles. The coatings show no change in impedance magnitude at 1 kHz when subject to 32 h of clinically relevant charge balanced current stimulation.

Introduction

Neural prosthetic devices aim to restore motor, sensory or cognitive function lost through physical injury or neurological disorder. The cochlear implant, for example, provides functional hearing by electrically stimulating neural tissue within the inner ear.[1,2] Crucial to the clinical success of these devices is the formation of a functional electrode–neural tissue interface that is stable over the intended lifetime of the device.

Neural prosthetic electrodes (NPEs) are commonly constructed from noble metals such as platinum, gold or iridium,[3] owing to their good electrical conductivity, electrochemical stability and biological inactivity. These materials, however, exhibit a number of shortcomings which limit device performance *in vivo*.[4,5] Slippage and micromotion of the electrode at its implantation site is thought to cause chronic inflammation because of disparity in mechanical properties between the electrode and host neural tissue.[6] Inflammatory events initiate encapsulation of the electrode within a sheath of scar tissue, decreasing the neuronal density at the electrode[3] and increasing the distance across which stimulation and recording currents must be transduced,[7,8] both of which are detrimental to the device performance. Furthermore, inert noble metal NPEs bear little biochemical resemblance to the neural tissue and therefore are not conducive to amiable tissue–electrode interaction. A more biologically compatible electrode could incorporate bioactive agents to mediate interactions at the interface, including anti-inflammatory agents to attenuate astroglial scarring events,[9–12] chemo-attractants to encourage neural outgrowth towards the electrode[13–16] and/or tethered cell adhesion motifs to promote cell anchorage to the electrode surface.[14,17,18]

Conducting polymer (CP) electrode coatings are potential components of more sophisticated NPEs. They undergo oxidative and reductive chemical processes accompanied by changes in a range of mechanical and electrical properties.[19] Oxidised polypyrrole features mobile, positively charged states responsible for electrical conductivity along the polymer backbone, which are electrostatically stabilised by the presence of dopant anions incorporated during synthesis. Upon reduction, these charged states are extinguished and either mobile dopant anions are expelled from the CP matrix, or cations are incorporated if the dopant anion is immobile.[20] This process may be reversed and is the mechanism by which CPs transduce electrical currents within neural prosthetic devices into ionic currents within the extracellur fluid of neural tissue (and *vice versa*). Two CPs with demonstrated biocompatibility and properties amendable to this application are polypyrrole (PPy)[21,22] and poly(3,4-ethylenedioxythiophene) (PEDOT).[23] Electrochemical synthesis of CPs enables site specific deposition of coatings onto the NPE surface and increases the electroactive surface area available for charge transfer. The choice of dopant species incorporated during synthesis presents an opportunity to dictate the electrical, mechanical, topological and bioactive properties of the coatings.[14,19] Furthermore, the use of polyelectrolyte dopants (including biopolymers) provides a means for further chemical modification of the coatings, imparting specific biochemical characteristics.

[a]*ARC Centre of Excellence for Electromaterials Science, Intelligent Polymer Research Institute, University of Wollongong, Wollongong, Australia. E-mail: gwallace@uow.edu.au; panhuis@uow.edu.au; Fax: +61 24221 4287; Tel: +61 24221 3155*
[b]*Soft Materials Group, School of Chemistry, University of Wollongong, Wollongong, Australia*

This journal is © The Royal Society of Chemistry 2011

Recently gellan gum (GG), a biologically derived polysaccharide, has emerged as a suitable hydrogel for tissue engineering[24,25] and drug delivery applications.[26] It is produced commercially by anaerobic fermentation of the bacterium *Sphingomonas elodea*.[27] In the presence of mono- or divalent cations, gellan gum forms ionically cross-linked hydrogel architectures.[25,28] Chemical deacylation can be used to modify the rheological properties of GG hydrogels from weak gels to gels of considerable strength.[29] GG has received US Food and Drug Administration and European Union (E418) approval for use in food and medicinal preparation, and is more commonly used as a thickening and stabilizing agent within the food industry.[30] Structurally, GG consists of a tetrasaccharide repeat unit, containing β-D-glucose, β-D-glucuronic acid and α-L-rhamnose monomers in a 2 : 1 : 1 ratio.[31] This resembles the carbohydrate component of glycosaminoglycans, a major component of the natural extracellular matrix. Glycosaminoglycans are fundamental to a range of cellular and tissue functions.[32] Carboxylic acid groups on the glucuronic acid residues enable aqueous solubility, and importantly, allow its incorporation within CP matrices as the charge-balancing dopant. Other extracellular matrix polysaccharides such as heparin[33] and hyaluronic acid[21,34] have been used previously to form CP based tissue engineering materials. Here, we report the synthesis of polypyrrole electrode coatings doped with gellan gum and explore their potential as NPE coatings in bionic and neural regeneration applications.

Experimental

Solution preparation

Gellan gum (Gelzan CM, $M_w = 5 \times 10^5$ Da) was a gift from CP Kelco. Solutions of GG (up to 1.5% w/v) were prepared by adding GG to Milli-Q water (18 MΩ cm) and stirring for 90 min at 80 °C. Pyrrole was sourced from Merck and distilled prior to use. GG–pyrrole solutions were prepared by adding pyrrole (0.25 M) to GG solutions at room temperature with stirring, while purging with N_2 gas.

Electrode coating preparation

PPy/GG coated electrodes were synthesised galvanostatically using a three-electrode electrochemical cell. Platinum mesh and Ag/AgCl electrodes were used as auxiliary and reference electrodes respectively. Gold-coated Mylar working electrodes (Delta Technologies) with an active area of 1 cm^2 were cleaned prior to use using surfactant solution, Milli-Q water and ethanol. Polymerisation was carried out at room temperature using a Model 363 Princeton Applied Research Potentiostat/Galvanostat and eDAQ Model 401 E-corder and eDAQ Chart software (version 5.2.11). Galvanic polymerisation conditions included current densities up to 4.0 mA cm^{-2} applied for up to 30 min. The resulting coated electrodes were rinsed with Milli-Q water.

Characterisation techniques

Electrochemical impedance spectroscopy (EIS) was carried out using a Gamry Impedance System, by subjecting coated electrodes to a 10 mV perturbation at a bias of 0 V, where PPy is in its oxidised state and not subject to substantial redox activity. The resulting currents and phase angles were measured at 20 points/decade over a frequency range between 100 kHz and 0.1 Hz. All measurements were carried out at room temperature in phosphate buffered saline (PBS, pH 7.4) electrolyte. Auxiliary and reference electrodes were as for PPy/GG electrode coating synthesis.

Cyclic voltammograms were obtained using the same three-electrode electrochemical cell set-up as for synthesis, using EChem Software (version 2.0.14). Redox behaviour of the PPy/GG coatings was examined over the potential window −0.8 V to +0.4 V at a scan rate 20 mV s^{-1}. Electrochemical stability of the coated electrodes was assessed over 400 cycles from −0.8 to +0.4 V, −0.45 to +0.2 V and −0.100 to 0.15 V, at a scan rate of 100 mV s^{-1}.

Simulated neural stimulation experiments were carried out by connecting four replicate PPy/GG coated electrodes and a gold-coated Mylar control electrode in series to form a total 5 cm^2 working electrode, positioned within a two-electrode electrochemical cell. This set-up allowed stimulation of multiple electrodes under identical conditions. Stainless steel mesh was used as the auxiliary and a pseudo-reference electrode, with PBS as the electrolyte. All experiments were conducted at room temperature. A 250 Hz biphasic, charge balanced current waveform was applied to the cell for a total of 32 h using an A310 Accupulser with an A365 Stimulus Isolator (World Precision Instruments, USA). Current amplitude and pulse width were 0.25 mA cm^{-2} and 100 μs respectively. The voltage developed within the system was measured using an E-corder 401 and eDAQ Chart software. An additional four unstimulated replicates were placed in PBS for the duration of the experiment. Impedance measurements were obtained for both stimulated and unstimulated electrodes at 8 h intervals up to 32 h.

Electrode coating surfaces were characterised using a Jeol 7500FA scanning electron microscope (SEM). Samples were prepared by drying at 40 °C for 24 h, and gold coated using an Edwards AUTO 306 Sputter coater system.

All of the results provided within this manuscript are the calculated mean values ± 1 standard deviation.

Results and discussion

Preparation of electrode coatings

Electrode coatings were prepared by galvanostatic electropolymerisation of pyrrole (0.25 M) in the presence of the anionic polyelectrolyte GG. At low (≤0.1% w/v) and high (≥0.5% w/v) polyelectrolyte concentrations, coating formation was not observed. This can be attributed to insufficient electrolyte conductivity[35] and viscosity limited reactant diffusion[21] respectively. Polymerization was successful in the GG concentration range 0.1%–0.5% w/v, and 0.25% w/v was selected for further characterisation of films.

Chronopotentiograms (Fig. 1) showed that at 0.1 mA cm^{-2} a potential of 0.6 V is drawn. This is generally considered the lower limit at which oxidation of polypyrrole will occur.[36] Higher current densities resulted in increases in initial potential, which steadily decreased with time. This is indicative that the working electrode–electrolyte interfacial resistance is decreasing, owing to

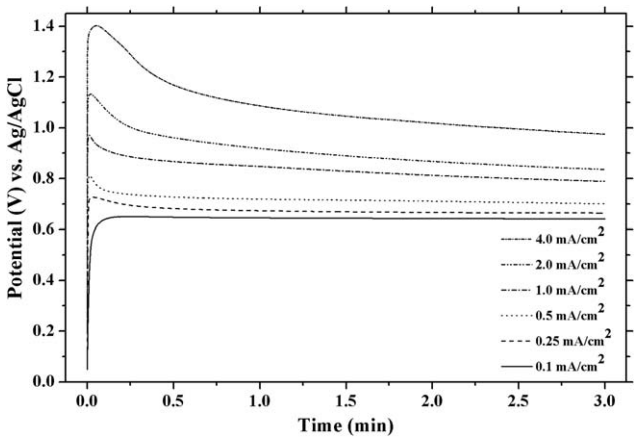

Fig. 1 Chronopotentiograms over the first 3 min of electropolymerisation of PPy/GG electrode coatings at various current densities.

an increasing electroactive surface area attributed to polymer deposition. The use of polyelectrolyte dopants is known to mitigate CP deposition.[35]

The use of high current densities (1.0 to 4.0 mA cm^{-2}) resulted in the deposition of a primary black PPy/GG layer, as well as an overlying secondary hydrogel layer (Fig. 2). We suggest that localised proton generation accompanying pyrrole polymerisation and increased GG chain concentration at the working electrode (by electrophoretic migration) is responsible for this hydrogel formation.[37] The gel thickness increased with both current density and polymerisation time. The secondary gel layer presents an interesting electrode structure for neural applications. Control over the gel layer may be used to facilitate the formation of an effective electrode–cellular interface. To control its formation, current densities were restricted to 0.25 mA cm^{-2} for all subsequent electropolymerisation reactions. The potential generated at this current density is only slightly higher than for 0.1 mA cm^{-2} (~0.6 V), where CP deposition was unsuccessful (Fig. 1). Therefore, this current density is close to the minimum required to cause CP deposition.

A range of polymerisation times of up to 30 min at the current density of 0.25 mA cm^{-2} were explored. SEM micrographs (Fig. 3) of PPy/GG coatings revealed that the surface morphology of PPy/GG differs from the nodular, cauliflower-like morphology more commonly observed for electropolymerised PPy films.[21,38] Low deposition charges (37.5 mC cm^{-2}, Fig. 3a) result in sub-micron sized islands containing fibrillar features, which extend and coalesce with continued polymerisation (150 mC cm^{-2}) to form a porous, web-like coverage (Fig. 3b). Further analysis (inset, Fig. 3b) revealed that the fibrillar structures vary between 10 nm and 100 nm in thickness, with a pore diameter in the range 10 to 500 nm. It is well-known that the type of dopant used during polymerisation profoundly affects the surface morphology.[38] Furthermore, the fibrillar network is similar to that observed for GG films and hydrogels by atomic force microscopy.[39,40] Therefore, it is likely that the observed GG/PPy surface morphology is induced by the GG network during polymerisation.

Fig. 2 Optical image of a PPy/GG coated electrode indicating the secondary GG hydrogel layer on top of the PPy/GG layer when current densities greater than 1 mA cm^{-2} were used.

Electrochemical characterisation of PPy/GG coated electrodes

Cyclic voltammetry and electrochemical impedance spectrometry were used to investigate the electrochemical characteristics of the PPy/GG coatings as a function of deposition charge. Coated electrodes were subject to a scanning potential from −0.8 to +0.4 V. This encompasses both the reduction and oxidation reactions of polypyrrole, without causing over-oxidation or reduction of dissolved oxygen at low potentials. Oxidation and reduction peaks around −0.33 and −0.47 V were observed (Fig. 4), their broadness reflecting the porous nature of the coating nanostructure as confirmed by SEM (Fig. 3). The

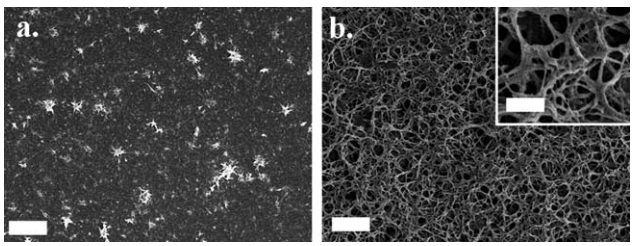

Fig. 3 SEM images of PPy/GG coatings on Au Mylar substrates polymerised at 0.25 mA cm^{-2}. The deposition charges were 37.5 mC cm^{-2} (a) and 150 mC cm^{-2} (b). Scale bars in (a) and (b) represent 1 μm, and 500 nm for the inset.

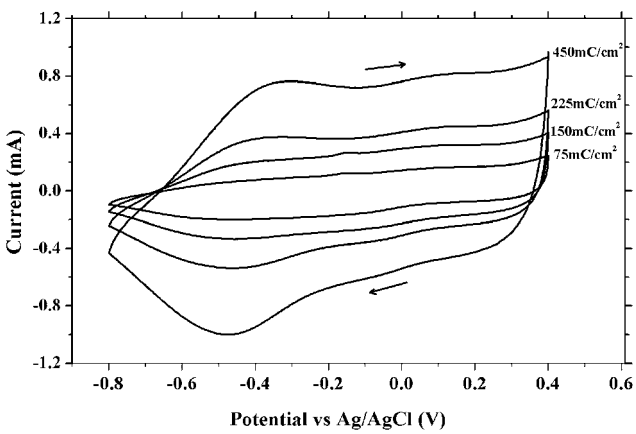

Fig. 4 Cyclic voltammograms of PPy/GG coated electrodes prepared with polymerisation times of 5, 10, 15 and 30 min at 0.25 mA cm^{-2}, equivalent to deposition charges of 75, 150, 225 and 450 mC cm^{-2}. The scan rate was 20 mV s^{-1}.

This journal is © The Royal Society of Chemistry 2011

increase in current magnitude for coatings produced with higher deposition charges indicates that a larger number of charged sites were available for charge transfer.

The effect of electrode surface modification on interfacial charge transfer is of fundamental interest for stimulation and recording of excitable tissues. Electrochemical impedance measurements were performed at a bias of 0 V, where the CP is in its oxidised, electrically conducting state. Impedance measurements demonstrated a significant reduction in impedance magnitude ($|Z|$) at frequencies lower than 1.2 kHz for PPy/GG coatings, compared to gold coated Mylar (Fig. 5a). At the lowest frequency tested (0.1 Hz), the films prepared with 37.5 mC cm^{-2} deposition charge exhibited two orders of magnitude reduction in $|Z|$, and films prepared using 450 mC cm^{-2} deposition charge showed three orders of magnitude reduction. Similar trends have been previously reported for other CP electrode coatings.[21,22,41] Improvements in interfacial charge transfer have been attributed to an increase in the electroactive surface area of the electrodes.[42] The porous surface morphology of PPy/GG coated electrodes is therefore likely to play a significant role in the improved impedance behaviour.

The impedance magnitude at 1 kHz, which is relevant to neural stimulation and recording applications, is often cited for the purpose of NPE comparison.[22] The favourable charge transfer characteristics imparted by PPy/GG coatings is apparent when the $|Z|$ at 1 kHz (24 ± 3 Ω) is compared to that of other polypyrrole coatings prepared in our laboratories, and reported previously.[43] The impedance magnitude at 1 kHz of PPy/GG is 45% lower than that of the lowest previously reported film, *p*-toluenesulfonic acid (pTS) doped PPy ($|Z| = 44$ Ω). Minimisation of impedance at the electrode–neural tissue interface is desirable as it reduces the charge injection required to stimulate neural tissue, minimising the impact on biological tissues and reducing power consumption. Low impedance also improves the sensitivity of neural recordings. The low impedance of these coated

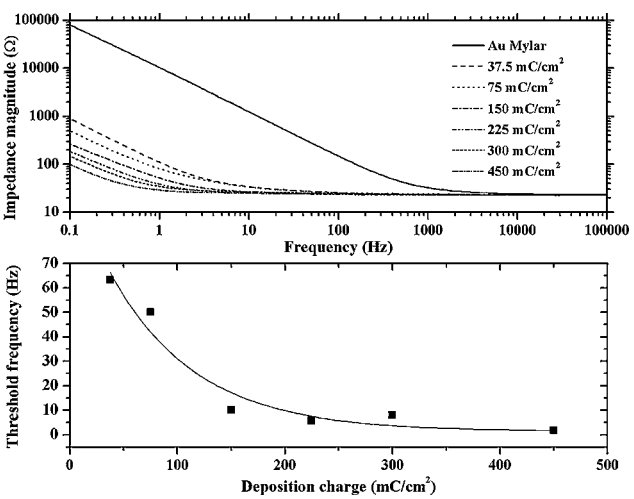

Fig. 5 (a) Impedance magnitude of PPy/GG electrodes as a function of perturbation frequency for deposition charges between 37.5 mC cm^{-2} and 450 mC cm^{-2}. The impedance of an uncoated Au Mylar electrode is shown for comparison. (b) The threshold frequency value (where impedance magnitude becomes independent of frequency) for PPy/GG coated electrodes prepared using 0.25 mA cm^{-2}. The solid line is an exponential fit to the data ($R^2 = 0.93$).

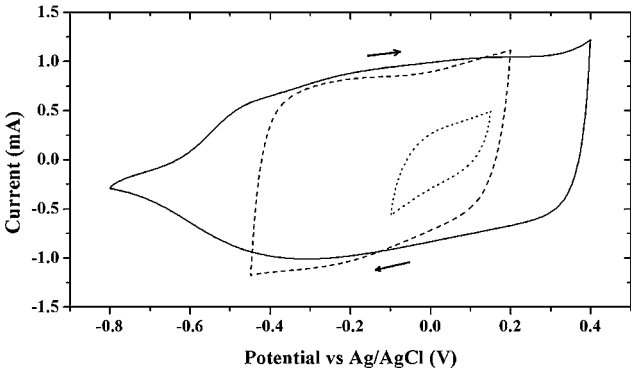

Fig. 6 Cyclic voltammograms of PPy/GG coated electrodes prepared using 150 mC cm^{-2} deposition charge. Large (−0.80 to +0.40 V, solid line), medium (−0.45 to +0.20 V, dashed line) and small (−0.10 to 0.15 V, dotted line) potential ranges were explored. Scans were obtained at 100 mV s^{-1} starting at the negative end of each potential window.

electrodes in the 10 Hz region suggests that these electrodes may also be suitable as scaffold components for the engineering of skeletal muscle tissue, which is responsive to lower frequencies than for neural tissue.[44]

Longer polymerisation times lead to an increase in the frequency range over which the impedance is independent of frequency. For example, for a polymer deposition charge of 450 mC cm^{-2}, $|Z|$ is independent of frequency between 1 Hz and 100 kHz. Thus the working range of these electrodes comfortably encompasses the frequencies at which neural cells transfer signals (100 Hz to 10 kHz[45]). Frequency-independent electrochemical characteristics are desirable for the interpretation of recordings from neural tissue. The threshold frequency at which $|Z|$ becomes independent of frequency decreased exponentially with deposition charge (Fig. 5b). It is apparent that deposition charges greater than ~150 mC cm^{-2} do not provide significant further improvements in frequency-independent impedance characteristics. Coatings prepared for subsequent stability studies had a deposition charge of 150 mC cm^{-2}.

Electrochemical stability studies

For functional NPEs, it is essential that the mechanism of charge transfer be reversible and stable over the intended lifetime of the device. The electrochemical stability of our coated electrodes was assessed using (i) potentiodynamic cycling and (ii) current pulse stimulation similar to that used in the stimulation of neural ganglion cells through cochlear implant electrodes.[46]

Table 1 The decrease in charge carrying capacity (Q_c) as a result of poteniodynamic cycling for 400 cycles. PSS indicates polystyrenesulfonate. $n = 4$ for PPy/GG coatings

CP coating	Loss of Q_c (%)	Ref.	Potential window/V	Scan rate/mV s^{-1}
PEDOT/pTS	10	47	−0.7 to 0.6	120
PPy/PSS + PEDOT/pTS	20	47	−0.7 to 0.6	120
PPy/gellan gum	23 ± 2	This paper	−0.8 to 0.4	100
PPy/PSS	61	48	−0.7 to 0.6	100
PPy/PSS	62	47	−0.7 to 0.6	120
PPy/PSS	100	49	−0.9 to 0.5	100

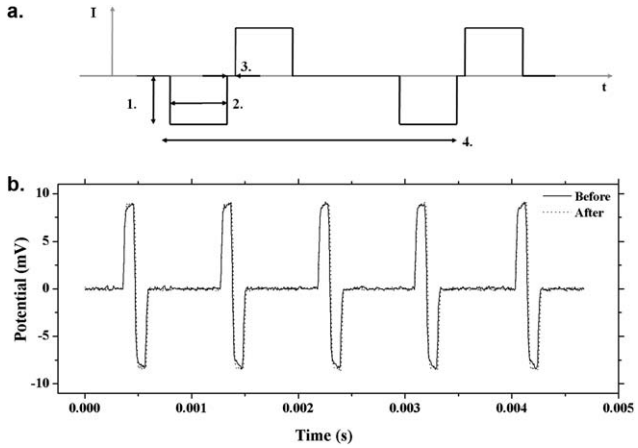

Fig. 7 (a) Schematic representation of the biphasic charge-balanced current waveform used to simulate neural stimulation. Numbered arrows 1–4 indicate pulse amplitude (0.25 mA cm^{-2}), pulse width (100 μs), interphase gap (10 μs), and event interval (4 ms) respectively. (b) Potential response of coated electrodes before (solid line) and after (dotted line) 32 h of biphasic pulsed current (current density = 0.25 mA cm^{-2}). Sections of the event interval have been truncated for clarity.

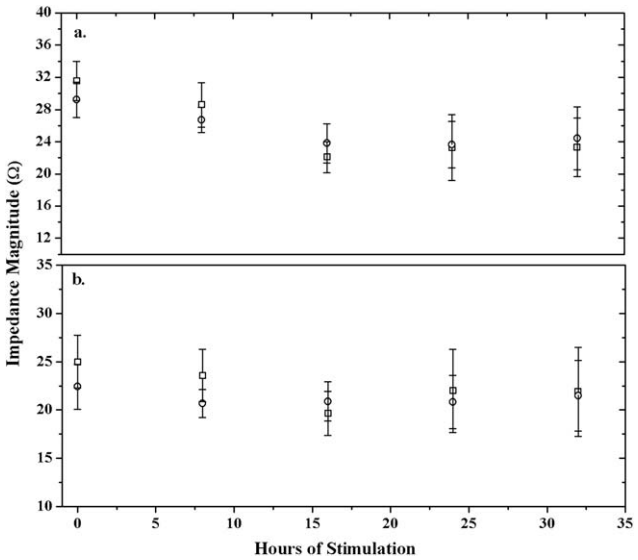

Fig. 8 Impedance magnitudes of PPy/GG coated electrodes (150 mC cm^{-2}) at (a) 250 Hz and (b) 1000 Hz, measured at 8 h intervals during biphasic pulsed current stimulation (squares) with comparison to unstimulated controls (circles).

PPy/GG coated electrodes were subjected to extended potentiodynamic cycling across three different potential windows (Fig. 6). The charge carrying capacity (area of the CV) was calculated after every 50 scans over a total of 400 scans. The charge-carrying capacity equates to the amount of charge crossing the electrode–electrolyte interface per scan. A decrease in this quantity over successive cycles suggests that the charge transduction mechanism is somewhat irreversible, indicating electrochemical instability within that potential range.[3,47] This approach has been used previously to provide insights into the electrochemical stability of other CP electrodes.[48–50] From the relative areas of the CV scans in Fig 6, it is clear that greater potential excursion enables substantially more charge to be passed during each scan. For the large potential window (−0.80 to +0.4 V), which includes both oxidation and reduction maxima, there was a gradual decrease in total charge passed as a function of cycle number, resulting in a 23 ± 2% decrease in charge carrying capacity over the 400 cycles. This relatively aggressive potential range is therefore detrimental to electrochemical performance. It has been suggested that irreversible expulsion of the dopant molecules from the CP may be provoked at large negative potentials, leading to reduced electroactivity.[35] It is also possible that slight over-oxidation of PPy is occurring on the positive sweep, resulting in reduced π-bond conjugation and decreased electrical conductivity. In comparison with similar results published previously, the electrochemical stability of PPy/GG is superior to PPy coatings doped with polystyrenesulfonate (PSS) and comparable to that of a layered structure of PPy/PSS and PEDOT/pTS (Table 1). The incorporation of large polyelectrolyte dopants (as opposed to smaller, more mobile dopants) has been shown to provide improved mechanical properties and lower susceptibility to degradation on CP reduction.[51,52] Superior stability of PEDOT/pTS coatings, with a loss of only 10% electroactivity, has been attributed to the dioxyethylene groups present at PEDOT's 3- and 4-positions, hindering nucleophilic attack which leads to the loss of conjugation.[53] No decrease in charge carrying capacity was encountered when potential was cycled within the two narrower potential windows over 400 cycles. This indicates that charge transduction is stable for the small potential excursions that are encountered during neural stimulation and recording (Fig. 7).

PPy/GG coatings were subjected to a 250 Hz biphasic pulsed-current stimulation waveform (Fig. 7a) for a total of 32 h. The maximum potential reached at the electrode was ±9 mV and this remained stable for the entire duration of stimulation (Fig. 7b). This is well within the stable working potential range of the electrodes determined using the potentiodynamic approach. The magnitude of impedance (as determined by EIS measurements) at both 250 Hz and 1 kHz was measured at 8 h intervals and compared to the impedance of unstimulated controls (Fig. 8). There was a good correlation between the impedances of stimulated and unstimulated samples, with no statistically significant change over 32 h of current pulsing. This suggests that PPy/GG coatings may be stable under physiologically relevant stimulation conditions.

Conclusions

In summary, gellan gum-doped polypyrrole electrode coatings significantly reduced the impedance encountered at frequencies relevant to neural cell communication, relative to uncoated gold electrodes. They are able to support clinically relevant stimulation over an extended period of time with no apparent decrease in performance. Accordingly, we have established that PPy/GG electrode coatings enhance the electrochemical characteristics of neural prosthetic electrodes, and as such may serve as an amenable platform for improvement of other important aspects of neural prosthetic electrodes. In particular, these include optimisation of mechanical and biochemical characteristics of the interface to improve cell–electrode interactions. This study

 This journal is © The Royal Society of Chemistry 2011

contributes to the development of emerging bioelectrode materials for neural prosthetic device applications.

Acknowledgements

The authors wish to thank the Australian Research Council (ARC) Federation Fellowship (G.G. Wallace), Future Fellowship (M. in het Panhuis), QEII Fellowship (Simon E. Moulton) and the Rotary Club of Kiama, Bill Wheeler Scholarship (T.M. Higgins) for their generous support. Mr Tony Romeo is thanked for assistance with SEM analysis.

Notes and references

1 T. E. Bell, K. D. Wise and D. J. Anderson, *Sens. Actuators, A*, 1998, **66**, 63–69.
2 G. M. Clark, *Clin. Exp. Pharmacol. Physiol.*, 1996, **23**, 766–776.
3 R. A. Green, N. H. Lovell, G. G. Wallace and L. A. Poole-Warren, *Biomaterials*, 2008, **29**, 3393–3399.
4 A. Branner, R. B. Stein, E. Fernandez, Y. Aoyagi and R. A. Normann, *IEEE Trans. Biomed. Eng.*, 2004, **51**, 146–157.
5 P. J. Rousche and R. A. Normann, *J. Neurosci. Methods*, 1998, **82**, 1–15.
6 H. Lee, R. V. Bellamkonda, W. Sun and M. E. Levenston, *J. Neural Eng.*, 2005, **2**, 81–89.
7 X. Cui, J. Wiler, M. Dzaman, R. A. Altschuler and D. C. Martin, *Biomaterials*, 2003, **24**, 777–787.
8 C. Newbold, R. Richardson, C. Q. Huang, D. Milojevic, R. Cowan and R. Shepherd, *J. Neural Eng.*, 2004, **1**, 218–227.
9 R. Wadhwa, C. F. Lagenaur and X. T. Cui, *J. Controlled Release*, 2006, **110**, 531–541.
10 W. Shain, L. Spataro, J. Dilgen, K. Haverstick, S. Retterer, M. Isaacson, M. Saltzman and J. N. Turner, *IEEE Trans. Neural Syst. Rehabil. Eng.*, 2003, **11**, 186–188.
11 Y. H. Zhong and R. V. Bellamkonda, *Brain Res.*, 2007, **1148**, 15–27.
12 W. He, G. C. McConnell, T. M. Schneider and R. V. Bellamkonda, *Adv. Mater.*, 2007, **19**, 3529–3533.
13 R. T. Richardson, B. Thompson, S. Moulton, C. Newbold, M. G. Lum, A. Cameron, G. Wallace, R. Kapsa, G. Clark and S. O'Leary, *Biomaterials*, 2007, **28**, 513–523.
14 D. Kim, S. M. Richardson-Burns, J. L. Hendricks, C. Sequera and D. C. Martin, *Adv. Funct. Mater.*, 2007, **17**, 79–86.
15 N. Gomez and C. E. Schmidt, *J. Biomed. Mater. Res., Part A*, 2006, **81**, 4–9.
16 S. J. Jhaveri, M. R. Hynd, N. Dowell-Mesfin, J. N. Turner, W. Shain and C. K. Ober, *Biomacromolecules*, 2009, **10**, 174–183.
17 L. M. Y. Yu, N. D. Leipzig and M. S. Shoichet, *Mater. Today*, 2008, **11**, 36–43.
18 E. Azemi, W. R. Stauffer, M. S. Gostock, C. F. Lagenaur and X. T. Cui, *Acta Biomater.*, 2008, **4**, 1208–1217.
19 G. G. Wallace, G. M. Spinks, L. A. Kane-Maguire and P. R. Teasdale, *Conductive Electroactive Polymers*, CRC Press, 3rd edn, 2009.
20 D. Zhou, C. O. Too and G. G. Wallace, *React. Funct. Polym.*, 1999, **39**, 19–26.
21 J. H. Collier, J. P. Camp, T. W. Hudson and C. E. Schmidt, *J. Biomed. Mater. Res.*, 2000, **50**, 574–584.
22 X. Cui, V. A. Lee, Y. Raphael, J. A. Wiler, J. F. Hetke, D. J. Anderson and D. C. Martin, *J. Biomed. Mater. Res.*, 2001, **56**, 261–272.
23 S. M. Richardson-Burns, J. L. Hendricks, B. Foster, L. K. Povlich, D. Kim and D. C. Martin, *Biomaterials*, 2007, **28**, 1539–1552.
24 A. M. Smith, R. M. Shelton, Y. Perrie and J. J. Harris, *J. Biomater. Appl.*, 2007, **22**, 241–254.
25 C. J. Ferris and M. in het Panhuis, *Soft Matter*, 2009, **5**, 3430.
26 T. R. Bhardwaj, M. Kanwar, R. Lal and A. Gupta, *Drug Dev. Ind. Pharm.*, 2000, **26**, 1025–1038.
27 P. A. Sandford, I. W. Cottrell and D. J. Pettitt, *Pure Appl. Chem.*, 1984, **56**, 879.
28 J. T. Oliveira, L. Martins, R. Picciochi, P. B. Malafaya, R. A. Sousa, N. M. Neves, J. F. Mano and R. L. Reis, *J. Biomed. Mater. Res., Part A*, 2010, **93**, 852–863.
29 R. Chandrasekaran and A. Radha, *Trends Food Sci. Technol.*, 1995, **6**, 143.
30 I. Giavasis, L. M. Harvey and B. McNeil, *Crit. Rev. Biotechnol.*, 2000, **20**, 177–211.
31 G. Ciardelli, V. Chiono, G. Vozzi, M. Pracella, A. Ahluwalia, N. Barbani, C. Cristallini and P. Giusti, *Biomacromolecules*, 2005, **6**, 1961–1976.
32 R. Lever, A. Smailbegovic and C. Page, *Inflammopharmacology*, 2001, **9**, 165–169.
33 J. S. Moreno, S. Panero, S. Materazzi, A. Martinelli, M. G. Sabbieti, D. Agas and G. Materazzi, *J. Biomed. Mater. Res., Part A*, 2009, **88**, 832–840.
34 K. J. Gilmore, M. Kita, Y. Han, A. Gelmi, M. J. Higgins, S. E. Moulton, G. M. Clark, R. Kapsa and G. G. Wallace, *Biomaterials*, 2009, **30**, 5292–5304.
35 G. G. Wallace, H. Zhao, C. O. Too and C. J. Small, *Synth. Met.*, 1997, **84**, 323–326.
36 D. D. Ateh, H. A. Navsaria and P. Vadgama, *J. R. Soc., Interface*, 2006, **3**, 741–752.
37 J.-I. Horinaka, K. Kani, Y. Hori and S. Maeda, *Biophys. Chem.*, 2004, **111**, 223–227.
38 G. G. Wallace, G. M. Spinks, L. A. P. Kane-Maguire and P. R. Teasdale, *Conductive Electroactive Polymers*, CRC Press, USA, 3rd edn, 2009.
39 A. P. Gunning, A. R. Kirby, M. J. Ridout, G. J. Brownsey and V. J. Morris, *Macromolecules*, 1996, **29**, 6791–6796.
40 V. J. Morris, A. R. Kirby and A. P. Gunning, *Scanning*, 1999, **21**, 287–292.
41 X. Cui, J. F. Hetke, J. A. Wiler, D. J. Anderson and D. C. Martin, *Sens. Actuators, A*, 2001, **93**, 8–18.
42 Y. Xiao, X. Cui and D. C. Martin, *J. Electroanal. Chem.*, 2004, **573**, 43–48.
43 X. Liu, K. J. Gilmore, S. E. Moulton and G. G. Wallace, *J. Neural Eng.*, 2009, **6**, 1.
44 G. Goldspink, *J. Anat.*, 1999, **194**, 323–334.
45 E. Valderrama, P. Garrido, E. Cabruja, P. Heiduschka, A. Harsch and W. Gopel, *Proceedings of the International Solid-State Sensors and Actuators Conference*, 1995, 63–66.
46 C. Newbold, R. Richardson, C. Q. Huang, D. Milojevic, R. Cowan and R. Shepherd, *J. Neural Eng.*, 2004, **1**, 218–227.
47 J. Yang and D. C. Martin, *Sens. Actuators, A*, 2004, **113**, 204–211.
48 R. A. Green, L. A. Poole-warren and N. H. Lovell, *Proceedings of the 3rd International IEEE/EMBS Conference on Neural Engineering*, 2007, 97–100.
49 R. A. Green, C. M. Williams, N. H. Lovell and L. A. Poole-Warren, *J. Mater. Sci.: Mater. Med.*, 2008, **19**, 1625–1629.
50 X. Cui and D. C. Martin, *Sens. Actuators, B*, 2003, **89**, 92–102.
51 X. Ren and P. G. Pickup, *J. Phys. Chem.*, 1993, **97**, 5356–5362.
52 H. Zhao and G. G. Wallace, *Polym. Gels Networks*, 1998, **6**, 233.
53 K. A. Ludwig, J. D. Uram, J. Yang, D. C. Martin and D. R. Kipke, *J. Neural Eng.*, 2006, **3**, 59–70.